

Effect of annealing on the optical constants of ZnO nanowires for energy harvesting applications

E. MUCHUWENI^{a,b,*}, T. S. SATHIARAJ^a, M. T. MAGAMA^b, P. DZOMBA^c

^aDepartment of Physics and Astronomy, Botswana International University of Science and Technology (BIUST), P. Bag 16, Palapye, Botswana

^bDepartment of Physics and Engineering, Bindura University of Science Education (BUSE), P. Bag 1020, Bindura, Zimbabwe

^cDepartment of Chemistry, Bindura University of Science Education (BUSE), P. Bag 1020, Bindura, Zimbabwe

The effect of annealing temperature on the optical constants of hydrothermally prepared ZnO nanowires was investigated for potential application in the fabrication of solar energy harvesting devices. Annealing at 150 °C led to an increase in the visible region refractive index and decrease in the extinction coefficient, which both exhibited an opposite trend at 250 – 350 °C. This was attributed to the initial increase in scattering and decrease in absorption of incident light at 150 °C, which then reversed its behaviour at 250 – 350 °C. The refractive index was around 1.9 – 2.3, while the extinction coefficient was around 0.01 – 0.10 in the visible range. These values were relatively higher than those of the gallium and aluminium co-doped ZnO (GAZO) thin films used as seed layers, which gave rise to the relatively lower transmittances observed for the ZnO nanowires. Other optical constants such as the effective single oscillator energy (E_o), dispersion energy (E_d), static dielectric constant (ϵ_0), static refractive index (n_0) and the nonlinear refractive index (n_2) were determined. The highest figure of merit of $3.6 \times 10^{-2} \Omega^{-1}$ was determined at 250 °C which demonstrated the significance of annealing in tailoring the optoelectronic properties of ZnO nanowires for application in solar energy harvesting device fabrication.

(Received June 10, 2019; accepted April 9, 2020)

Keywords: ZnO, Nanowires, Optical constants, Figure of merit, Annealing temperature

1. Introduction

The bulk and thin film forms of ZnO have been widely studied since the 1950s. However, with the recent advances in technology, an assortment of ZnO nanostructures such as nanorings, nanoflowers, nanowires and nanotubes have gained more research attention due to their novel properties [1, 2]. Among these, ZnO nanowires are more attractive due to their quantum confinement effects and diversity for potential device application [3, 4].

ZnO nanowires exhibit a single crystalline structure with less grain boundaries and defects which gives them better optoelectronic properties than those of bulk ZnO and thin films [5]. ZnO nanowires have large surface-to-volume ratios which make them more attractive for energy harvesting in solar cell structures [6, 7] and piezoelectric nanogenerators [8]. Their bio-safety, bio-degradability and low fabrication cost enable them to be used for biomedical applications such as efficient photocatalysts to inactivate viruses and bacteria, and for the degradation of environmental pollutants [9, 10]. Their high refractive index facilitates usage in optical waveguide applications, especially as optical nano-fibers [11]. The ability to control their nucleation sites makes them suitable for the fabrication of micro-lasers and memory array devices [3]. ZnO nanowires can also be used in photoelectrochemical cells as n-type photoanodes for water splitting applications [12, 13].

ZnO nanowires are commonly grown using the hydrothermal synthesis technique. However, this synthesis route usually produces nanowires with relatively poor crystallinity and high defect density [14-16]. Therefore, it is vital to tune the hydrothermal growth parameters and post-synthesis annealing conditions so as to achieve favourable properties [17-19].

ZnO nanowires annealed in air at various temperatures have been reported previously [20]. However, the study did not go as far as determining their optical constants and figure of merit (FOM), which if investigated provide crucial information with regards to the nanowires' optoelectronic performance. The present study therefore, expands the previous work by reporting for the first time, the optical constants and FOM of ZnO nanowires annealed at various temperatures for use as potential candidates in the fabrication of solar energy harvesting devices.

2. Experimental details

ZnO nanowires were hydrothermally grown and annealed in air at 150 – 350 °C as described elsewhere [20]. Their optical transmittance was measured using a double beam UV/Vis/NIR spectrophotometer (Lambda-750, Perkin-Elmer, USA) with a resolution of

0.17 – 5.00 nm in the 300 – 800 nm wavelength region. Samples were mounted with the coated side directed towards the light source, so as to prevent the reflection that would occur if the uncoated smooth glass surface was the one facing towards the light source. The reference beam played a vital role in setting the baseline correction by removing the absorption effect of the glass substrate and was considered as 100% transmission. During the baseline correction and all measurements, no sample was mounted on the reference path.

The optical transmittance data was used to determine the refractive index (n) and extinction coefficient (k) through theoretical modelling using the Optichar software, version 11.65. The obtained values of n and k were then used to determine the single oscillator dispersion energies (E_o and E_d), static refractive index (n_0), nonlinear refractive index (n_2) and the Urbach energy (E_u).

The electrical resistivity was determined at room temperature from four-point probe resistivity measurements using an EZ GP-4303 power supply, a Signatone probe and two Keithley 197 digital multimeters. Since this work is an expansion of a previous study, the other characterizations by X-ray diffraction (XRD), Raman spectroscopy, field-emission scanning electron microscopy (FE-SEM) and Hall effect measurements, can be found in ref [20].

3. Results and discussion

Fig. 1 shows the transmittance spectra of ZnO nanowires as a function of annealing temperature, as presented and discussed elsewhere [20]. This was used in the present work to determine the refractive index and extinction coefficient through optical modelling.

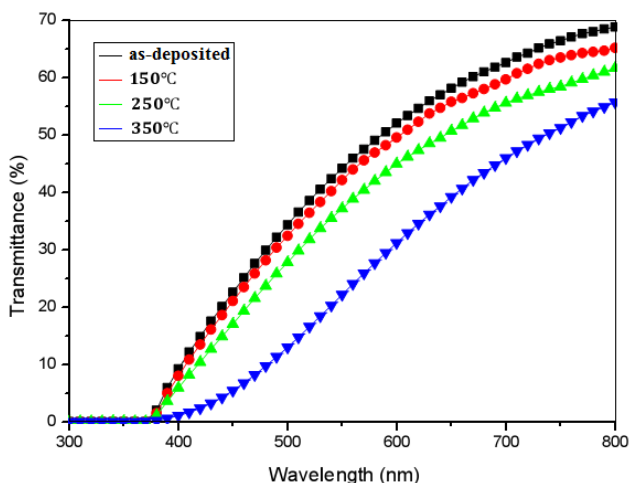


Fig. 1. The transmittance spectra of as-deposited and annealed ZnO nanowires [20] (color online)

Figs. 2 and 3 show the spectral dependence of the refractive index and extinction coefficient with annealing

temperature, respectively. Annealing at 150 °C led to an increase in the visible region refractive index and decrease in the extinction coefficient. A further increase in annealing temperature to 250 – 350 °C, however, resulted in a decrease in the visible region refractive index and an increase in the extinction coefficient. This observed trend was associated with the variations in the surface morphology of the samples, reported in a previous study [20]. The refractive index and extinction coefficient values were respectively around (1.9 – 2.3) and (0.01 – 0.10) in the visible region. These values were slightly greater than those for the GAZO thin films [21], used as seed layers. This demonstrated that the ZnO nanowires had relatively higher reflection and absorption coefficients which make them attractive for use in light scattering and collection devices. This also corroborated the relatively lower transmittances observed for the ZnO nanowires than for the GAZO thin film seed layers [21].

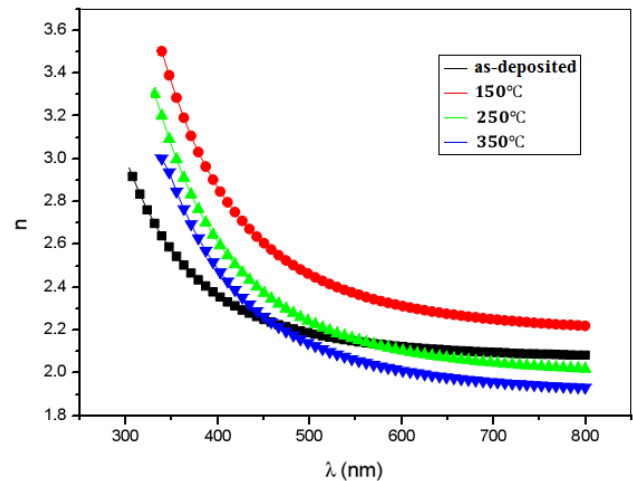


Fig. 2. The refractive index of ZnO nanowires as a function of annealing temperature (color online)

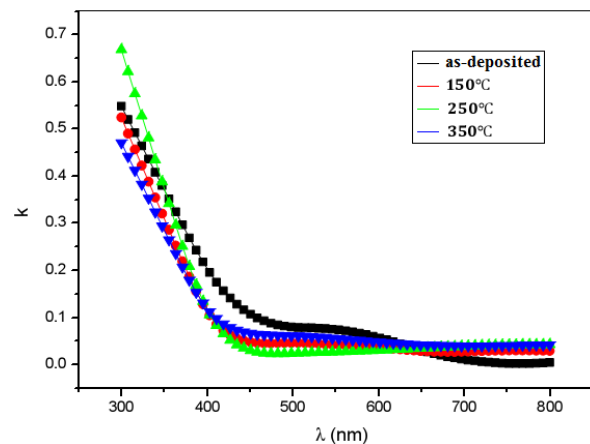


Fig. 3. The extinction coefficient of ZnO nanowires as a function of annealing temperature (color online)

The Wemple and DiDomenico (WDD) single oscillator model was used to determine the variation of refractive index with photon energy in the low absorption region, by plotting Fig. 4 which shows the variation of $(n^2 - 1)^{-1}$ with $(hv)^2$. This was used to determine the effective single oscillator energy (E_o) and dispersion energy (E_d) from the slope $\left(\frac{1}{E_o E_d}\right)$ and intercept $\left(\frac{E_o}{E_d}\right)$. The

obtained values of E_o and E_d were listed in Table 1 and were used to estimate the static dielectric constant (ϵ_0) and static refractive index (n_0) using the equation [22]:

$$n_0 = \sqrt{1 + \frac{E_d}{E_o}} = \sqrt{\epsilon_0} \quad (1)$$

Table 1. The variation of E_o , E_d , ϵ_0 , n_0 , $\chi^{(1)}$, $\chi^{(3)}$, n_2 and E_u with annealing temperature.

Annealing temperature (°C)	E_o (eV)	E_d (eV)	ϵ_0	n_0	$\chi^{(1)}$	$\chi^{(3)}$ ($\times 10^{-13}$ esu)	n_2 ($\times 10^{-12}$ esu)	E_u (meV)
As-deposited	6.15	19.88	1.44	2.06	0.26	7.44	13.62	556
150	6.58	24.22	1.47	2.16	0.29	12.51	21.84	346
250	6.38	18.31	1.40	1.97	0.23	4.62	8.85	301
350	6.50	16.54	1.37	1.88	0.20	2.86	5.73	404

The obtained values of E_o , E_d , ϵ_0 and n_0 were comparable to those obtained in other studies [23-25]. Annealed samples had higher E_o values than the as-deposited samples. This demonstrated a reduction in residual stress and improvement in crystallinity [26], in good agreement with Raman spectroscopy and XRD analysis reported in a separate study [20]. E_d , ϵ_0 and n_0 firstly increased and then decreased at higher annealing temperature which was attributed to the transition of the sample microstructure, firstly to a more ordered phase and then to a randomly oriented phase [26]. This was consistent with FE-SEM analysis reported in a previous study [20].

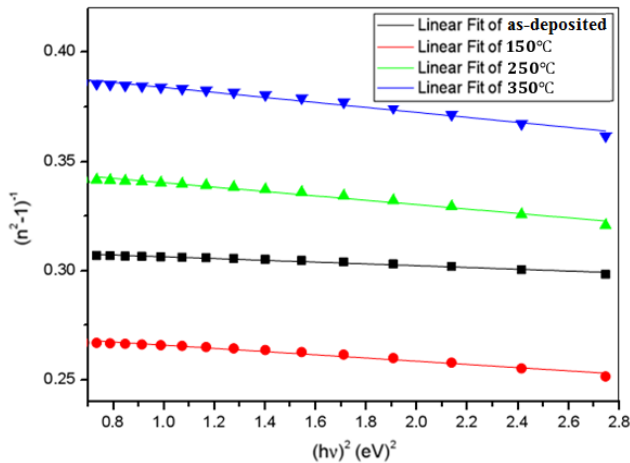


Fig. 4. A plot of $(n^2 - 1)^{-1}$ versus $(hv)^2$ for the ZnO nanowires annealed at different temperatures (color online)

Nonlinear effects are experienced when light of high intensity traverses through a medium [26, 27]. The incident intensity greatly affects the non-linear refractive index (n_2) which is given by the Tichý and Tichá relation [28]:

$$n_2 = \frac{12\pi\chi^{(3)}}{n_0} \quad (2)$$

where n_0 is the static refractive index and $\chi^{(3)}$ is the third order non-linear susceptibility which is approximated in the long wavelength region by the generalized Miller's rule:

$$\chi^{(3)} = A[\chi^{(1)}]^4 \quad (3)$$

where $A = 1.7 \times 10^{-10}$ esu and $\chi^{(1)}$ is the linear susceptibility, given by:

$$\chi^{(1)} = \frac{E_d}{4\pi E_o} \quad (4)$$

Therefore, $\chi^{(3)}$ is given as:

$$\chi^{(3)} = \frac{A(n_0^2 - 1)^4}{(4\pi)^4} \quad (5)$$

The values of $\chi^{(1)}$, $\chi^{(3)}$ and n_2 were listed in Table 1. They showed an increasing trend with annealing temperature up to 150 °C and decreased thereafter in good agreement with the linear refractive index and other studies [26, 27].

The Urbach energy (E_u) was determined from the reciprocal of the slope of the linear fit of $\ln\alpha$ versus hv , shown in Fig. 5, and the obtained values were recorded in Table 1. All annealed samples had relatively lower E_u values than the as-deposited samples which demonstrated the significance of annealing in reducing the concentration of structural defects and disorder. The minimum value of E_u was determined after annealing at 250 °C which was attributed to the optimum structural and morphological properties, in good agreement with XRD and FE-SEM analysis, reported elsewhere [20].

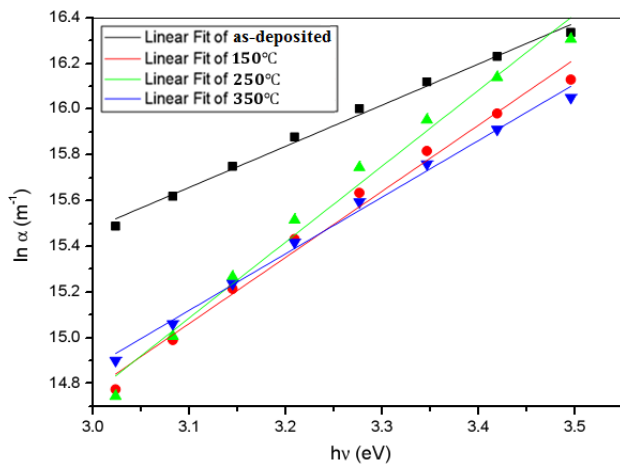


Fig. 5. A plot of $\ln\alpha$ versus $h\nu$ as a function of annealing temperature (color online)

The figure of merit (FOM) for the ZnO nanowires was calculated using the equation [29]:

$$FOM = \frac{1}{\alpha\rho} \quad (6)$$

where α is the absorption coefficient at 550 nm and ρ is the electrical resistivity. The obtained values were plotted in Fig. 6 as a function of annealing temperature.

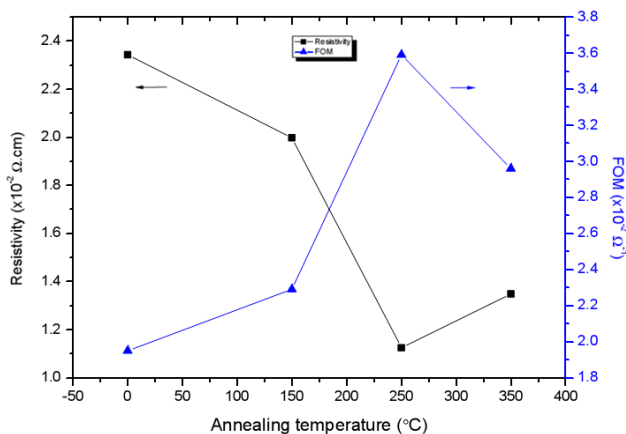


Fig. 6. The electrical resistivity and FOM for the as-deposited and $150 - 350\text{ }^\circ\text{C}$ annealed ZnO nanowires (color online)

All annealed samples had relatively higher figure of merit values as compared to their as-deposited counterparts, with the maximum value observed at $250\text{ }^\circ\text{C}$. This demonstrated the significance of annealing in producing a favourable combination of high visible optical transmittance and good electrical conductivity [30], which is required in high performance optoelectronic devices. Interestingly, the figure of merit values obtained in the present study were consistent with those reported in other

studies [31-34], indicating the suitability of the prepared ZnO nanowires for light collection and energy harvesting applications.

4. Conclusion

The refractive index and extinction coefficient of ZnO nanowires annealed at various temperatures were successfully determined through optical modelling. These were used to investigate the other optical constants such as the single oscillator dispersion energies, static refractive index and nonlinear refractive index as a function of annealing temperature. Desirable optoelectronic properties for solar energy harvesting applications were obtained in nanowires annealed at $250\text{ }^\circ\text{C}$ as demonstrated by their highest figure of merit.

Acknowledgements

This work was performed using the research facilities at Botswana International University of Science and Technology (BIUST).

References

- [1] J. Zhang, W. Que, Sol. Energ. Mater. Sol. Cells **94**, 2181 (2010).
- [2] Z. L. Wang, J. Phys.: Condens. Matter **16**, R829 (2004).
- [3] D. P. Singh, Sci. Adva. Mater. **2**, 245 (2010).
- [4] G.-C. Yi, C. Wang, W. I. Park, Semicond. Sci. Technol. **20**, S22 (2005).
- [5] M. C. Akgun, Y. E. Kalay, H. E. Unalan, J. Mater. Res. **27**, 1445 (2012).
- [6] J. Y. Chen, K. W. Sun, Sol. Energ. Mater. Sol. Cells **94**, 930 (2010).
- [7] M. Petrov, K. Lovchinov, D. Dimova-Malinovska, A. Ulyashin, Bulg. J. Phys. **40**, 229 (2013).
- [8] G. Poulin-Vittrant, C. Oshman, C. Opuku, A. S. Dahiya, N. Camara, D. Alquier, Phys. Procedia **70**, 909 (2015).
- [9] H. J. Zhou, S. S. Wong, ACS Nano **2**, 944 (2008).
- [10] C. Hariharan, Appl. Catal. A **304**, 55 (2006).
- [11] W. Yang, F. Wan, S. Chen, C. Jiang, Nanoscale Res. Lett. **4**, 1486 (2009).
- [12] S. U. M. Khan, M. Al-Shahry, W. B. Ingler, Science **297**, 2243 (2002).
- [13] X. Yang, A. Wolcott, G. Wang, A. Sobo, R. C. Fitzmorris, F. Qian, J. Z. Zhang, Y. Li, Nano Lett. **9**, 2331 (2009).
- [14] L. E. Greene, M. Law, J. Goldberger, F. Kim, J. C. Johnson, Y. F. Zhang, R. J. Saykally, P. D. Yang, Angew. Chem. Int. Ed. **42**, 3031 (2003).
- [15] J. Fan, Y. Hao, C. Munuera, M. García-Hernández,

- F. Güell, E. M. J. Johansson, G. Boschloo, A. Hagfeldt, A. Cabot, *J. Phys. Chem. C* **117**, 16349 (2013).
- [16] X. Q. Zhao, C. R. Kim, J. Y. Lee, C. M. Shin, J. H. Heo, J. Y. Leem, H. Ryu, J. H. Chang, H. C. Lee, C. S. Son, B. C. Shin, W. J. Lee, W. G. Jung, S. T. Tan, J. L. Zhao, X. W. Sun, *Appl. Surf. Sci.* **255**, 5861 (2009).
- [17] C. K. Xu, J. M. Wu, U. V. Desai, D. Gao, *J. Am. Chem. Soc.* **133**, 8122 (2011).
- [18] M. Law, L. E. Greene, J. C. Johnson, R. Saykally, P. Yang, *Nat. Mater.* **4**, 455 (2005).
- [19] C. K. Xu, J. M. Wu, U. V. Desai, D. Gao, *Nano Lett.* **12**, 2420 (2012).
- [20] E. Muchuweni, T. S. Sathiaraj, H. Nyakoty, *Mater. Sci. Eng. B* **227**, 68 (2018).
- [21] E. Muchuweni, T. S. Sathiaraj, J. Masanganise, N. Muchanyereyi, J. Inorg. Organomet. Polym. *Mater.* **29**, 48 (2019).
- [22] D. Komaraiah, E. Radha, Y. Vijayakumar, J. Sivakumar, M. V. R. Reddy, R. Sayanna, *Mod. Res. Catal.* **5**, 130 (2016).
- [23] F. Yakuphanoglu, S. Ilican, M. Caglar, Y. Caglar, *J. Optoelectron. Adv. M.* **9**, 2180 (2007).
- [24] S. K. Ahmmad, M. A. Samee, A. Edukondalu, S. Rahman, *Results Phys.* **2**, 175 (2012).
- [25] A. Bedia, F. Z. Bedia, M. Aillerie, N. Maloufi, B. Benyoucef, *Energy Procedia* **50**, 603 (2014).
- [26] G. Malik, J. Jaiswal, S. Mourya, R. Chandra, *J. Appl. Phys.* **122**, 143105 (2017).
- [27] E. R. Shaaban, M. El-Hagary, El. –S. Moustafa, H. S. Hassan, Y. A. M. Ismail, M. Emam-Ismail, A. S. Ali, *Appl. Phys. A.* **122**, 20 (2016).
- [28] H. Tichá, J. Schwarz, L. Tichý, R. Mertens, *J. Optoelectron. Adv. M.* **6**, 747 (2004).
- [29] G. Haacke, *J. Appl. Phys.* **47**, 4086 (1976).
- [30] A. R. Babar, P. R. Deshamukh, R. J. Deokate, D. Haranath, C. H. Bhosale, K. Y. Rajpure, *J. Phys. D* **41**, 135404 (2008).
- [31] C. Muiva, T. S. Sathiaraj, K. Maabong, *Mater. Sci. Forum* **706**, 2577 (2012).
- [32] E. Muchuweni, T. S. Sathiaraj, H. Nyakoty, *Ceram. Int.* **42**, 10066 (2016).
- [33] E. Muchuweni, T. S. Sathiaraj, H. Nyakoty, *Heliyon* **3**, e00285 (2017).
- [34] E. Muchuweni, T. S. Sathiaraj, H. Nyakoty, *Mater. Sci. Semicond. Process.* **68**, 80 (2017).

*Corresponding author: muchuweniedigar1@gmail.com